



**HAL**  
open science

## Genomic characterization of viruses associated with the parasitoid *Anagyrus vladimiri* (Hymenoptera: Encyrtidae)

Yehuda Izraeli, David Lepetit, Shir Atias, Netta Mozes-Daube, Gal Wodowski, Oded Lachman, Neta Luria, Shimon Steinberg, Julien Varaldi, Einat Zchori-Fein, et al.

### ► To cite this version:

Yehuda Izraeli, David Lepetit, Shir Atias, Netta Mozes-Daube, Gal Wodowski, et al.. Genomic characterization of viruses associated with the parasitoid *Anagyrus vladimiri* (Hymenoptera: Encyrtidae). *Journal of General Virology*, 2022, 103 (12), 10.1099/jgv.0.001810 . hal-03896330

**HAL Id: hal-03896330**

**<https://hal.science/hal-03896330v1>**

Submitted on 3 Jan 2023

**HAL** is a multi-disciplinary open access archive for the deposit and dissemination of scientific research documents, whether they are published or not. The documents may come from teaching and research institutions in France or abroad, or from public or private research centers.

L'archive ouverte pluridisciplinaire **HAL**, est destinée au dépôt et à la diffusion de documents scientifiques de niveau recherche, publiés ou non, émanant des établissements d'enseignement et de recherche français ou étrangers, des laboratoires publics ou privés.

1 Cover page

2 **Genomic characterization of viruses associated with the parasitoid**

3 ***Anagyrus vladimiri* (Hymenoptera: Encyrtidae)**

4 **Yehuda Izraeli<sup>1,3</sup>, David Lepetit<sup>2</sup>, Shir Atias<sup>3</sup>, Netta Mozes-Daube<sup>3</sup>, Gal Wodowski<sup>1,3</sup>, Oded**  
5 **Lachman<sup>4</sup>, Neta Luria<sup>4</sup>, Shimon Steinberg<sup>5</sup>, Julien Varaldi<sup>2</sup>, Einat Zchori-Fein<sup>3</sup> and Elad**  
6 **Chiel<sup>\*6</sup>**

7 <sup>1</sup>University of Haifa, Department of Evolutionary and Environmental Biology, Haifa, Israel,

8 <sup>2</sup>Laboratoire de Biométrie et Biologie Evolutive, Université Lyon 1, CNRS, Villeurbanne,  
9 France,

10 <sup>3</sup>Newe Ya'ar Research Center, Department of Entomology, ARO, Ramat Yishai, Israel,

11 <sup>4</sup>Volcani Research Center, Department of Plant Pathology and Weed Research, ARO, Rishon  
12 LeZion, Israel

13 <sup>5</sup>BioBee Sde Eliyahu Ltd, Emek Hamaayanot, Israel

14 <sup>6</sup>University of Haifa – Oranim, Department of Biology and Environment, Tivon, Israel

15 **\* Correspondence:**

16 Elad Chiel

17 elad-c@sci.haifa.ac.il

18 **Keywords:** biocontrol agent, dicistrovirus, endosymbiont, iflavirus, mealybug, reovirus, virome

19 **Running title:** The Virome of a Biological Control Agent Parasitoid

## 20 Abstract

21 The knowledge on symbiotic microorganisms of insects has increased in recent years, yet  
22 relatively little data is available on non-pathogenic viruses. Here we studied the virome of the  
23 parasitoid wasp *Anagyrus vladimiri* (Hymenoptera: Encyrtidae), a biocontrol agent of mealybugs.  
24 By high-throughput sequencing of viral nucleic acids, we revealed three novel viruses, belonging  
25 to the families *Reoviridae* (provisionally termed AnvRV [*Anagyrus vladimiri* reovirus]),  
26 *Iflaviridae* (AnvIFV) and *Dicistroviridae* (AnvDV). Phylogenetic analysis further classified the  
27 AnvRV in the genus *Idnoreovirus*, and the AnvDV in the genus *Triatovirus*. The genome of  
28 AnvRV is comprised of 10 distinct genomic segments ranging in length from 1.5 to 4.2 Kbp, but  
29 only two out of the 10 open reading frames (ORFs) have a known function. AnvIFV and AnvDV  
30 each have one polypeptide ORF, which is typical to iflaviruses but very un-common among  
31 dicistroviruses. AnvRV was found to be fixed in a mass-reared population of *A. vladimiri*, whereas  
32 it's prevalence in field-collected wasps was ~15%. Similarly, the prevalence of AnvIFV and  
33 AnvDV were much higher in the mass rearing population than in the field population.  
34 Transmission electron micrographs of females' ovaries revealed clusters and viroplasm of  
35 *Reovirus*-like particles in follicle cells. AnvRV was not detected in the mealybugs, suggesting that  
36 this virus is truly associated with the wasps. The possible effects of these viruses on *A. vladimiri*'s  
37 biology, and on biocontrol agents in general are discussed. Our findings identify RNA viruses as  
38 potential players involved in the multitrophic system of mealybugs, their parasitoids and other  
39 members of the holobiont.

## 40 Importance

41 Different biological control approaches use industrially mass-reared natural enemy insects to  
42 reduce damage of arthropod pests. Such mass-reared cultures may be positively and/or negatively  
43 affected by various microorganisms, including viruses. Yet, current knowledge on virus diversity,  
44 especially in arthropods, is limited. Here, we provide the first virome characterization of a member  
45 of the wasps family Encyrtidae - the member being the parasitoid *Anagyrus vladimiri* - a  
46 commercially important natural enemy of mealybug pests. We describe the genome of three  
47 previously unknown RNA viruses, co-inhabiting this parasitoid, and elaborate on the prevalence  
48 of those viruses in individual wasps of both mass-reared and environmental origins. Microscopy  
49 images suggest that at least one of the viruses is transmitted maternally via the ovaries. We discuss

50 the genomic structure of the viruses and the possible relationship between those viruses and the *A.*  
51 *vladimiri* host, with implications on improvement of biocontrol of mealybug pests.

## 52 Introduction

53 Numerous arthropod species host symbiotic microorganisms that are integral to their life history,  
54 ecology and evolution (Zchori-Fein and Bourtzis, 2011). Such microorganisms engage in a wide  
55 range of symbiotic relationships, from parasitism to obligate mutualism, and may affect various  
56 biological features of their hosts (Zchori-Fein and Bourtzis, 2011; Drew et al., 2021). While the  
57 diverse interactions of bacteria, and to a lesser extent of fungi, with insects have been extensively  
58 studied, viruses associated with insects are much less explored. This is mainly due to paucity of  
59 knowledge of a great fraction of virus diversity as attested by recent large-scale or more focused  
60 surveys that unravelled numerous new virus lineages (Shi et al., 2016; Webster et al., 2016; Wu et  
61 al., 2020).

62 Among insects, it appears that endoparasitoids have special relationships with viruses. Those  
63 insects develop within an arthropod host, ultimately causing its death (Godfray, H. J., 1994). Most  
64 parasitoids belong to the order Hymenoptera. Apart from pathogenic viruses, they often harbour  
65 inherited viruses that may affect their phenotype. For instance, some viruses may affect their  
66 behaviour, as observed in the solitary parasitoid *Leptopilina boulardi*. In that case, the virus forces  
67 infected females to superparasitize (i.e., laying eggs in already parasitized hosts), thus favouring  
68 its horizontal transmission within the superparasitized host (Varaldi et al., 2003, 2005). The ssRNA  
69 iflavirus DcPV is also injected by the parasitoid *Dinocampus coccinellae* into its ladybeetle host  
70 during oviposition. The virus then replicates in the beetle's brain which may participate in turning  
71 the ladybeetle into a 'zombie' that guards the parasitoid cocoon from predation (Dheilly et al.,  
72 2015). Other true free-living viruses, such as the entomopoxvirus DIEPV found in some parasitoid  
73 wasps, may protect the wasp offspring from host immune reaction (Coffman et al., 2020). On the  
74 farther end of the pathogenic-mutualist axis, are some domesticated viruses that became integrated  
75 into the insect genome. The best-known example of this phenomenon is the case of polydnviruses  
76 (PDVs) which are associated with wasps that parasitize caterpillars of butterflies and moths. The  
77 endogenized viral genes allow the production of viral-like particles which are injected together  
78 with the eggs inside the caterpillar host and suppress its immune system, hence allowing the  
79 successful development of the wasp larvae (Herniou et al., 2013). Evidently then, viruses have

80 diverse and important effects on the phenotype and ecology of endoparasitoids, and there are likely  
81 many more virus-insect associations that are yet to be unveiled. In the current study the viruses  
82 associated with *Anagyrus vladimiri* Triapitsyn (Hymenoptera: Encyrtidae), a solitary  
83 endoparasitoid wasp attacking mealybugs (Hemiptera: Pseudococcidae), were identified and  
84 characterized. *Anagyrus vladimiri* is mass-reared for commercial use in biological control  
85 programs to manage two major global pest species, which attack plants in dozens of families: the  
86 citrus mealybug, *Planococcus citri* (Risso) and the vine mealybug *P. ficus* (Signoret) (Bugila et  
87 al., 2015). The female parasitoid lays an egg into the body of the mealybug host, which continues  
88 to develop while the wasp larva feeds and develops inside it. After a few days the mealybug host  
89 dies, its cuticle hardens and turns into a ‘mummy’ and the parasitoid larva pupates inside.  
90 Eventually, the adult parasitoid chews a hole in the mummified host and emerges (Avidov et al.,  
91 1967).

92 Recently, we reported an analysis of the fungal and bacterial portion of microbiome inhabiting this  
93 population of *A. vladimiri*. We found that the symbiont *Wolbachia* is dominating the bacterial  
94 community and under some conditions it has minor negative effects on the fecundity of the  
95 parasitoid (Izraeli et al., 2020). The current research was launched to characterize the virome of *A.*  
96 *vladimiri*, annotate the viral genomes, assess their phylogenetic position, and test the prevalence  
97 of the various viruses in lab and field populations of the wasp.

## 98 Results

### 99 *Electrophoresis characterization of Anagyrus vladimiri virome*

100 Viral nucleic acids (VNAs) were purified from a pool of adults (from the mass-reared line, see  
101 Table 1 for details) and treated by RNaseA and DNaseI. At least nine bands ranging in size from  
102 ~1.5Kbp to ~4Kbp were clearly observed when VNAs were separated on non-denaturing gel by  
103 electrophoresis (Fig. 1, lane 3). VNAs were successfully digested by RNaseA (Fig. 1, lanes 8-11),  
104 but not by DNaseI (Fig. 1, lanes 13), suggesting that the virome of *A. vladimiri* is composed of  
105 RNA viruses only. For both our positive control (Phi6 dsRNA) and the VNAs from *A. vladimiri*,  
106 the RNase digestion was mitigated in high concentration of sodium citrate buffer (=high ionic  
107 strength) with low concentration of RNase, which is the expected outcome when the RNA is  
108 double-, and not single-stranded (Sorrentino et al., 1980; Khramtsov et al., 1997). These results  
109 suggest that the tested strain of *A. vladimiri* harbours at least one, dsRNA virus with nine segments  
110 (or more, since segments of similar size may co-migrate at the same position), or several non-  
111 segmented or segmented dsRNA viruses.

### 112 *Sequencing the RNA virome of A. vladimiri*

113 After reverse transcription, the VNAs of *A. vladimiri* were sequenced on an Illumina platform. We  
114 obtained 16 million of high quality paired-end reads. High sequence duplication levels were  
115 observed (>96%), suggesting that the genome sequence is complete (except for the extremities of  
116 untranslated regions), and as expected from the apparent low complexity of the sample (Fig. 1)  
117 which totalled approximately 20-30Kbp. De novo assembly of this dataset, resulted in only 30  
118 contigs, 18 of which were shorter than 1,500bp.

119 Homology (by amino acid sequence identity) of 11 out of the 12 contigs longer than 1,500bp, as  
120 identified by BLASTx and PSI-BLASTp, were found to three RNA virus families; *Dicistroviridae*,  
121 *Iflaviridae* (both positive strand ssRNA, order: *Picornavirales*) and *Reoviridae* (segmented linear  
122 dsRNA, order: *Reovirales*) (Table 2, Fig. 2).

123 One contig was most similar to a *Dicistroviridae* member named Black queen cell virus infecting  
124 honeybees, with an average of 41% amino acid sequence identity. The contig is 8,726bp long,  
125 which is in the expected range for *Dicistriviridae* in general (8.5-10.2kb) and very close to the  
126 genome length of Black queen cell virus (8,550bp). We propose to name this newly discovered  
127 virus: *Anagyrus vladimiri dicistrovirus* (AnvDV).

128 One contig, 10,031bp long, had the highest similarity to different members of the family  
129 *Iflaviridae*, with 46% amino acid identity with the iflavirus member *Dinocampus coccinellae*  
130 paralysis virus used as a reference. The contig length is well within the expected range for  
131 *Iflaviridae* (8.8-9.7kb). We propose to name this newly discovered virus: Anagyrus vladimiri  
132 iflavirus (AnvIFV).

133 Nine contigs were identified as homologous to nine different segments of a reovirus infecting the  
134 winter moth *Operophtera brumata* (ObIRV). Protein alignment to the known ObIRV segments as  
135 a reference by BLASTp, revealed that the coverage between the nine contigs to the nine segments  
136 ranges between 20-98%, while the amino acid sequence identity ranges between 19% and 37% in  
137 all segments (Table 2). The one remaining contig out of the 12 ‘long’ ones, had no similarity  
138 according to BLASTx and Psi-BLASTp searches (contig k199\_18). However, its length was  
139 similar to other contigs assigned to the reovirus, therefore it was added to the screening assay for  
140 all reovirus segments in individuals. Results of that assay (see below) strongly support the  
141 assumption that this contig is part of the reovirus genome, and together with the nine contigs  
142 identified by BLAST, this genome consists of 10 segments. We propose to name this newly  
143 discovered segmented virus: Anagyrus vladimiri reovirus (AnvRV).

144 Six out of the 18 contigs shorter than 1,500bp (contigs k119\_1, k119\_3, k119\_5, k119\_8, k119\_9  
145 and k119\_13; Fig. 2), were also assigned to the *Iflaviridae* family by the BLASTx search (Table  
146 2, Fig. 2). Aligning those to the long AnvIFV contig showed that the small contigs are actually  
147 parts of this long contig with >96% nucleotide identity. They were discarded from the analysis.

148 The nearly-complete genome sequence of the three novel RNA viruses is available in GeneBank  
149 under BioProject PRJNA641546, with the following BioSample accession numbers \_\_\_.

#### 150 *Annotation*

151 Analysis of the recovered contigs predicted that all 12 ‘long’ (>1,500bp) ones have a large open  
152 reading frame (ORF), covering >90% of their length, suggesting that they encode true functional  
153 genes. In contrast, most of the 18 ‘short’ (<1,500bp) contigs had large portions of un-translated  
154 regions (UTRs), with the ORFs covering on average less than 60% (Table 2, Fig. 2).

155 Interestingly, the contig identified as AnvDV harbours only one ORF, unlike most known viruses  
156 of this family, which harbour two ORFs. Furthermore, no ‘internal ribosome entry site’ (IRES) -  
157 an RNA element typically found between the two ORFs of dicistroviruses (and enables the  
158 translation initiation of the second ORF) - was found along this contig. The genomes of the three

159 RNA viruses were further annotated by searching the predicted ORFs for conserved domains using  
160 the NCBI CDD tool. Both the AnvIFV and AnvDV were found to each harbour five domains  
161 encoding for: RNA-dependent RNA polymerase (RdRP) (accession: cd01699), RNA helicase  
162 (accession: pfam00910), capsid proteins (CRPV\_capsid superfamily, found in many  
163 dicistroviruses) (accession: cl07393) and two ‘rhv-like’ domains (part of a capsid protein, named  
164 as ‘drug-binding pocket’ found in poliovirus, also a member of *Picornavirales* order) (accession:  
165 cd00205) (Fig. 3a).

166 No conserved domains were found for the 10 AnvRV segments. Nevertheless, two genes were  
167 inferred from the BLASTx searches by homology with the ObIRV genome: RdRP on segment  
168 no.1 and a polyhedrin protein on segment no.4 (Fig. 3b).

169 One conserved sequence motif (GAAGAKC) was found in the 3’ end termini of the five out of 10  
170 contigs assigned to AnvRV (supp. fig 2). No conserved sequences were found in the 5’ end,  
171 suggesting that a few bases in the extremities of the contigs may be missing in our current  
172 assembly.

### 173 *Phylogeny*

174 *AnvRV*. Phylogenetic analysis of the RdRP encoding segment of the AnvRV revealed that its  
175 closest known relative is the ‘Zoersel tick virus’, identified from the tick *Ixodes ricinus*. This virus,  
176 together with three other close relatives, have no genus taxonomic classification. The closest  
177 classified virus is the ObIRV, which belongs to the genus *Idnoreovirus* (Fig. 4). Pairwise  
178 alignments of the AnvRV to those five viruses reveals a 34-43% RdRP amino acid sequence  
179 identity, while it’s amino acid identity with all other viruses compared in the phylogenetic analysis  
180 was 27% and lower. As the common cut-off between ICTV verified genera is 30% amino acid  
181 identity (Matthijssens et al., 2022), this suggests that the AnvRV, together with the four other  
182 unclassified relatives, belongs to the genus *Idnoreovirus* (Fig. 4).

183 *AnvDV*. The phylogenetic analysis for the AnvDV clearly show that this virus belongs to the genus  
184 *Triatovirus*, together with the Black queen cell virus (51% amino acid RdRP identity) and other  
185 relatives (Fig. 5).

186 *AnvIFV*. The phylogenetic analysis for the AnvIFV place this virus near the *Nasonia vitripennis*  
187 virus [accession ACN94442.1], *Aedes vexans* iflavirus [QGW51140.1](61-62% amino acid RdRP  
188 identity), and others. The unique *Dinocampus coccinellae* paralysis virus [YP\_009111311.1], also  
189 clusters on the same branch with AnvIFV, and has 58% amino acid RdRP identity with it (Fig. 5).



190 *Prevalence of viruses in lab and field samples*

191 To assess the prevalence of the three RNA virus candidates in the different *A. vladimiri*  
192 populations, diagnostic PCRs with specific primers were used (Supp. table 1) on 20 individual  
193 females from each of the *Wolbachia*-carrying ( $W^+$ ) and *Wolbachia*-free ( $W^-$ ) lab-reared lines  
194 (Izraeli et al., 2020). In addition, 24 field-collected individuals were screened (see Table 1 for  
195 details).

196 All 40 lab-reared individuals harboured the AnvRV. The AnvIFV and the AnvDV were found in  
197 33 and 25 specimens out of 40 individuals respectively (Fig. 6). All three viruses were also detected  
198 in field individuals, although the prevalence was lower, with three females carrying AnvRV  
199 (12.5%), 10 carrying AnvDV (42%), and two carrying AnvIFV (8%) out of 24 individuals (Fig.  
200 6).

201 Interestingly, out of 10 field females carrying the AnvDV, only three lacked *Wolbachia*, and seven  
202 out of the eight females carrying *Wolbachia*, also carried the AnvDV. The co-occurrence of those  
203 two microbes was statistically significantly correlated (Fisher's exact test:  $p=0.002$ ), suggesting a  
204 positive interaction between *Wolbachia* and AnvDV within *A. vladimiri* populations. However,  
205 AnvDV was present both in the *Wolbachia* positive and the *Wolbachia* negative strains in the lab.

206 *Screening for the 10 Reovirus segments in individual A. vladimiri wasps*

207 To test whether all the 10 Reovirus segments (nine identified by sequence homology, and one -  
208 contig K119\_18 - suspected by its length and UTR/contig length ratio) belong to the same AnvRV  
209 genome, rather than to different RNA viruses, 24 individuals from two wasp lines were screened  
210 by a set of diagnostic PCRs. Those included 16 individuals from the  $W^+RV^+$  line - a line harbouring  
211 the AnvRV as confirmed by PCR with primers targeting the RdRP segment, and 8 individuals  
212 from the 'Field-RV-' line, as negative controls. Generally, the results were as expected (table 3);  
213 in 9  $W^+RV^+$  individuals all the segments were amplified, while in 6 'Field-RV-' individuals, none  
214 were amplified, suggesting that all 10 segments belong to the same virus. However, in 7  
215 individuals, one or two segments failed to amplify, and in two individuals from the negative  
216 population one single segment was detected (Table 3).

217 *Presence of viruses in the mealybugs*

218 To test whether any of the three RNA viruses originated from the mealybug hosts, four pools were  
219 tested for their presence: i) Mass-reared (MR)  $W^+$  *A. vladimiri*, ii) Field-collected *A. vladimiri* line  
220 without the AnvRV ( $RV^-$ ), iii) un-parasitized *P. citri*, and iv) *P. citri*, four days after parasitization

221 by MR *A. vladimiri*, (see Table 1 for details). AnvRV was not detected in the un-parasitized  
222 mealybugs, nor in the Field-RV<sup>-</sup> *A. vladimiri*, which were reared under the same conditions as the  
223 MR *A. vladimiri*, indicating that this virus was not acquired from the mealybugs, and is associated  
224 with *A. vladimiri*. In contrast, AnvIFV and AnvDV were detected in both *A. vladimiri* and un-  
225 parasitized mealybugs (albeit the bands for the mealybug samples were weak, they were confirmed  
226 by Sanger sequencing, with >99% identity), suggesting that those viruses may be acquired from  
227 the mealybugs or from the rearing environment, possibly the potato sprouts that the mealybugs  
228 feed on (Cheng et al., 2021), or even the various fungi that develop on this substrate  
229 (supplementary Fig. 1).

### 230 *Virus particles in A. vladimiri ovaries*

231 To validate the presence of viruses in the females' reproductive tissues, transmission electron  
232 microscopy (TEM) was carried on sections of *A. vladimiri* ovaries (from the W<sup>+</sup>RV<sup>+</sup> line, see Table  
233 1 for details). Images obtained from the three specimens tested showed clusters of round shaped  
234 viral particles, 60-65nm in diameter, organized either in viroplasm structures, or in dense clusters  
235 in the perinucleus area in the cytoplasm of follicle cells (Fig. 7). This pattern is typical to  
236 *Reoviridae* viruses (Shah et al., 2017).

## 237 Discussion

238 The viral community of the parasitoid *A. vladimiri*, an agriculturally important biological control  
239 agent of mealybugs, is dominated by two positive ssRNA viruses from the order *Picornavirales*,  
240 which have sequence similarity to viruses of economically important insects, and a dsRNA  
241 segmented genome, assigned to the *Idnoreovirus* genus of the *Reoviridae* family. The latter was  
242 localized in the ovaries of the *A. vladimiri*, and was not found in the mealybug hosts, suggesting it  
243 specifically infects the wasp.

244 As most insect viromes are yet to be explored, it was not surprising to discover new viruses in this  
245 host (e.g. Shi et al. 2016). Nevertheless, to the best of our knowledge, other than this study there  
246 is only one available detailed report on viruses in wasps of the family Encyrtidae, which reported  
247 the genome sequence of one Picorna-like virus in the parasitoid *Diversinervus elegans* (Wu et al.,  
248 2021).

249 Most reoviruses reported to infect insects were found in Dipterans and in Lepidopterans (most of  
250 them in species that are important agricultural pests), and are assigned to the genera *Cypovirus* (16  
251 accepted species, which include >75 isolates), and *Idnoreovirus* (7 accepted species, >10 isolates)  
252 (Matthijnsens et al., 2022). Some are reported to cause chronic diarrheal disease to larvae, with  
253 mild-severe symptoms, while many others have no apparent symptoms on their host  
254 (Matthijnsens et al., 2022).

255 Out of the few reports on reoviruses infecting parasitoids, even fewer have tested for phenotypic  
256 effects of the virus on its host. Renault et al., (2005) and Graham et al., (2008) both found no  
257 evidence for phenotypic effects of reoviruses inhabiting *Diadromus pulchellus* and *Phobocampe*  
258 *tempestiva* respectively. However, in some cases, reoviruses evidently cause significant effects on  
259 their parasitoid host. Renault et al., (2003) reported that during parasitization *Diadromus*  
260 *pulchellus* females inject a reovirus into the lepidopteran host together with the egg, where like the  
261 PDV effect, it inhibits the immune response and allows the full development of the parasitoid  
262 larva. In contrast, the cypovirus that infects both *Campoletis sonorensis* parasitoid and its  
263 lepidopteran host (in which it cannot replicate), seems to be beneficial to the lepidopteran as it  
264 reduces percent of mortality from parasitism (Deacutis, 2012).

265 Viruses of the families *Dicistroviridae* (15 accepted species, which include many more isolates)  
266 and *Iflaviridae* (15 accepted species, >80 isolates) are more commonly associated with insects, but  
267 similarly to reoviruses, in most cases their phenotype in the insect host is unknown (Valles et al.,  
268 2017a, 2017b). Reported effects of viruses from those families are mostly pathogenic (e.g., Acute  
269 bee paralysis virus, Drosophila C virus, Cricket paralysis virus, for *Dicistroviridae*, and Varroa  
270 destructor virus1, Deformed wing virus for *Iflaviridae*). Conversely, at least one symbiotic  
271 relationship of those viruses with parasitoids was reported. The iflavirus DcPV aids the  
272 *Dinocampus coccinellae* to paralyze its ladybeetles host, as it replicates in the ladybeetle brain  
273 possibly leading to behaviour changes that protect the developing parasitoid (Dheilly et al., 2015).  
274 Another symbiotic relationship was found between a cripavirus (*Dicistroviridae*) and *Drosophila*  
275 flies, where the virus seems to increase the fecundity of individuals that carry it (Zhang et al.,  
276 2021).

277 As mentioned above, in most cases the relationship of the virus with its insect host is unknown.  
278 As *A. vladimiri* wasps are reared in our lab for many generations, with no apparent disease  
279 symptoms, it can be assumed that under the tested rearing conditions (especially the AnvRV,

280 which is fixed in the mass-reared population), the virus is at least not pathogenic, or even may be  
281 beneficial to the wasp. Nonetheless, all scenarios are to be taken into consideration when  
282 speculating on the relationship of those three novel viruses with *A.vladimiri*, including the  
283 possibility that those viruses don't have any phenotypic effect, and are spread in the population  
284 through efficient vertical and or horizontal transmission (e.g. Lüthi et al., 2020; Martinez et al.,  
285 2016; Perreau & Moran, 2022) . Future study should address these possibilities.

286 Screening the wasp populations showed that while the two ssRNA viruses are not present in all  
287 individuals, the AnvRV is fixed in the lab-reared lines, suggesting either efficient transfer of this  
288 virus, whether vertical, horizontal or both (e.g. Varaldi et al., 2006). It may also suggest that the  
289 specific rearing conditions favour the carrying of the virus (e.g. Himler et al., 2011; Coffman et  
290 al., 2020). However, due to the low prevalence of the AnvRV in field populations of *A. vladimiri*,  
291 we conclude that the interaction between the two is not obligatory. Additionally, while the two  
292 ssRNA viruses were detected in virion extractions of unparasitized mealybugs, the AnvRV was  
293 not, meaning it is a wasp symbiont. On the other hand, the two ssRNA viruses may originate from  
294 the mealybug, or they can infect both the wasp and its host (e.g. Zhang et al., 2021)).

295 The TEM images of virus particles in follicle cells of *A. vladimiri*, resemble the typical pattern  
296 found in viruses from the family Reoviridae, which are known to be found in the cytoplasm, to be  
297 round shaped, 60-70nm long, and may be occluded in viroplasms (Shah et al., 2017). All species  
298 of this genus were detected only in insects (Matthijssens et al., 2022) .Such a localization of a  
299 microbe in the ovary, strongly suggests vertical maternal transfer, which in turn may hint on long  
300 evolutionary relationships, and perhaps mutualism, between the two (Zchori-Fein and Bourtzis,  
301 2011; Perlmutter and Bordenstein, 2020).

302 The evolutionary arms race between parasitoids and their hosts have led for several defence  
303 mechanisms that hosts use to escape parasitism. In response to invasion by an endo-parasitoid egg  
304 (or other foreign organisms), immune haemocytes in mealybugs may aggregate around the inserted  
305 egg, and form a melanized capsule, which eliminates its development (Blumberg, 1997). The rates  
306 of this encapsulation response to *A. vladimiri* parasitism is known to differ between *P. citri* and *P.*  
307 *ficus* hosts species (Blumberg et al., 1995; Suma et al., 2012). it can be speculated that AnvRV  
308 aids the wasp to overcome encapsulation, like DpRV2 does in the *Diadromus pulchellus* -  
309 *Acrolepiopsis assectella* system (Renault et al., 2003), but with different efficiency in different  
310 *Planococcus* hosts. If this speculation is indeed true then the different prevalence between lab and

311 field lines can be explained by the fact that the field population originated in vineyards where *P.*  
312 *ficus* is the main host for *A. vladimiri*, whereas the lab population develops in *P. citri* hosts.

313 Overall results of the screening of all ten segments in *A. vladimiri* specimens, were conclusive and  
314 indicate that all segments belong to the same virus. However, four segments failed to amplify in  
315 between one-four out of 16 specimens tested. This might suggest that those four segments have  
316 lower copy numbers than the other five. The detection of segment number four (k119\_19) in two  
317 specimens of the negative population can be explained by either technical error, or by  
318 contamination.

319 From the pattern of *Wolbachia* and AnVDV prevalence in the 24 field collected females, where the  
320 presence of those two microorganisms is somewhat correlated, it can be speculated that some  
321 interaction takes place between those two. Reports on *Wolbachia* interaction with viruses focus on  
322 associations with human viral pathogens vectored by insects and insect diseases caused by viruses.  
323 For example, *Wolbachia* protects *Drosophila* flies from the Drosophila C virus (Family:  
324 *Dicistroviridae*) (e.g. Hedges et al., 2008), and inhibits the Dengue Fever and Chikungunya  
325 pathogens in humans (DENV and CHIKV, both also positive ssRNA viruses), (e.g. Hoffmann et  
326 al., 2011; Walker et al., 2011). This effect is also detected in natural populations of *Drosophila*  
327 and is however virus-specific (Cogni et al., 2021). Those inhibitions were generally correlated with  
328 lower viral copy number of the viruses. In other cases, endosymbionts do correlate positively with  
329 viral presence and transmission (e.g. Gottlieb et al., 2010; Kliot et al., 2014), such as reported here  
330 for *A. vladimiri*, where a significant positive correlation was found between the presence of the  
331 bacterium and the AnVDV in the field population, and also a higher prevalence in the lab strain  
332 infected by *Wolbachia*. This is intriguing since it could suggest a positive effect of *Wolbachia* on  
333 virus transmission, may further indicate that this virus and *Wolbachia* interact and clearly needs to  
334 be further investigated.

335 Interestingly, in oppose to most species of Dicistroviridae members, which have a ‘Di-cistronic’  
336 genome (the trait which is the source of the family’s name), only one polypeptide ORF could be  
337 identified in AnVDV. This is more similar to other families in the *Picornavirales* order, such as  
338 *Iflaviridae* and *Picornaviridae*, however in those families the genes are in opposite order to the  
339 order that was found in the AnVDV, where non-structural proteins are closer to the 3’ end (Bonning  
340 and Miller, 2010). As far as we know, such genomic arrangement was found only in a few viruses,  
341 most of which are from aquatic invertebrates (Shi et al., 2016, see supplementary data #33; Cheng

342 et al., 2021; Wu et al., 2021). This rare finding suggests that this family has a broader diversity  
343 than previously known.

344

### 345 **Conclusion**

346 Most studies on viruses in insects focus on pathogenic interactions or transient in vectors to plants  
347 or animals. This is one of the first attempts to characterize the virome of a biocontrol agent, that  
348 overall seems to be healthy. The discovery of three new RNA viruses in a single population with  
349 no apparent diseases, highlights the richness of this hidden community of viruses. This community  
350 certainly deserves further investigation in order to clarify its transmission along generations and  
351 the phenotypic effects associated. If one (or more) of the three viruses influences the efficiency of  
352 *A. vladimiri* as a natural enemy, whether positively or negatively, this knowledge can be applied  
353 to improve the biological control of mealybug pests.

## 354 Methods

### 355 *Insect rearing and field collections of parasitoids*

356 *Anagyrus vladimiri* wasps were obtained from 'BioBee Sde Eliyahu Ltd' mass-rearing (MR)  
357 facility (Sde Eliyahu, Israel), and used to establish a *Wolbachia*-positive line ( $W^+$ ), from which a  
358 *Wolbachia*-free line ( $W^-$ ) was established by antibiotic treatments (Izraeli et al., 2020). The two  
359 lines were reared under controlled conditions of  $26\pm 1^\circ\text{C}$ ,  $60\pm 20\%$  RH, and 16L:8D photoperiod  
360 regime on the citrus mealybugs *Planococcus citri*, feeding on sprouted potatoes *Solanum*  
361 *tuberosum*.

362 Additional *A. vladimiri* individuals were collected in the field during the summer of 2020, using  
363 funnel insect traps placed in an unsprayed vineyard in northern Israel (32.7200N, 35.1903E). The  
364 traps ( $n=10$ ), baited with mealybugs-infested potatoes, were retrieved from the field after one week  
365 and parasitized mealybugs were incubated in the lab. The *A. vladimiri* adults which emerged  
366 (emergence was achieved from three out of the 10 traps, the other seven were empty), were used  
367 either for screening viruses' prevalence ( $n=24$ , results in Fig. 3), and others were let to parasitize  
368 in the lab, establishing the 'Field' line ( $n\sim 20$  female foundresses). One generation later, eight  
369 females of this Field line were individually placed in cups and allowed to oviposit in mealybugs.  
370 Mothers and three of their emerged offspring were then tested for the presence of the AnvRV and  
371 *Wolbachia*. All the cups in which both symbionts were not detected ( $n=7$ , since *Wolbachia* was  
372 detected in one mother) were pooled to establish an uninfected *A. vladimiri* line (termed hereafter  
373 'Field-RV-' line).

374 The origins of the five wasp lines, and the various experiments they were used for are summarized  
375 in Table 1.

### 376 *Enzymatic characterization of A. vladimiris' virome*

377 To characterize the viral community inhabiting *A. vladimiri*, viral nucleic acids (VNAs) were  
378 purified following (Martinez et al., 2016). Briefly, viral capsids were purified from 0.5 g of MR  
379 *A. vladimiri* wasps (pool of  $>1,500$  individuals), by filtration, nuclease treatment (RNaseA and  
380 DNaseI) and centrifugation. To classify the genome type of potential viruses (RNA/DNA,  
381 double/single strand), VNAs were then extracted by SDS, subjected to different nuclease  
382 treatments, and then examined on an 0.8% agarose gel (Martinez et al., 2016). A non-treated VNA

383 sample, a dsRNA ladder (Phi6, Invitrogen, MA, USA), and a DNA ladder (1Kb+, Invitrogen, MA,  
384 USA) were used as controls.

### 385 *Sequencing strategy*

386 To further reveal all viral candidates inhabiting the wasp, VNAs were extracted from purified viral  
387 capsids using the All-In-One DNA/RNA Miniprep Kit (Biobasic, ON, Canada). Since the gel  
388 images produced in this process showed no indication of viral DNA molecules, only samples with  
389 RNA VNAs were further examined and sequenced. Libraries were prepared by the TruSeq RNA  
390 Ribo-Zero kit (Illumina, CA, USA) and sequenced by Illumina novaseq 6000 with 100 bp paired-  
391 end reads.

392 Since the sequence yield was very high (~16 million paired-end reads, where suspected viruses'  
393 genome size is up to 30 thousand bp), the data was randomly subsampled to three smaller datasets,  
394 including  $10^5$  paired reads,  $10^6$  paired reads and  $2 \times 10^6$  paired reads. The subsampled datasets  
395 were *de-novo* assembled using 'Megahit' version 3.4 with default parameters. Comparing  
396 assembly results of the three subsampled datasets to the original full dataset, revealed that most of  
397 the contigs are identical, with a few additional small contigs and the  $10^6$  paired reads dataset was  
398 chosen as the most suitable for further analysis (average fold (sometimes termed 'depth') per bp =  
399  $4.2 \times 10^4$ ). The resulting contigs were searched for homologous similarity against both the nr and  
400 the swissprot databases using BLASTx, targeting viruses, bacteria and Hymenoptera (taxids  
401 10239, 2, 7399 respectively). The following parameters were changed from default to increase  
402 sensitivity: matrix – BLOSUM45, Gap costs – 12;2. An additional PSI-Blastp analysis, using the  
403 protein sequences predicted by the ORFfinder online tool (RRID:SCR\_016643), was used to  
404 identify similarity of contigs that Blastx failed to identify.

### 405 *Annotation*

406 All contigs were subjected to an open reading frame (ORF) search using ORFfinder online tool  
407 (RRID:SCR\_016643), with start codon including alternative initiation codons. The length of the  
408 un-translated regions (UTR), included the 5' and 3'UTRs, was calculated as contig length minus  
409 the ORF length. As the ORFfinder tool may predict also false proteins, a calculation of UTR  
410 divided by the contig length was done to estimate the likeliness of the contig to harbour a 'true'  
411 protein, the higher the value the lower chance to have a 'true' protein.



412 The UTRs of the ten identified segments of AnvRV were searched for conserved sequence motifs  
413 in the 5' and 3' end termini. This was done by subjecting those UTR sequences to a BLAST search  
414 against themselves, with the automatic adjusted parameters for short sequences of NCBI BLASTn  
415 suite.

416 Further annotation analysis of the viral genomes was done by subjecting all the ORFs to the NCBI  
417 batch-CDD tool (Marchler-Bauer et al., 2015) , against the CDD v.3.19 database to search for  
418 conserved domains. For relevant viruses a search for internal ribosome entry sites (IRES) was done  
419 by the IRESite online tool (IRESite: The database of experimentally verified IRES structures,  
420 2022) using the NUC4.4 matrix.

#### 421 *Phylogeny*

422 To construct phylogenetic trees of the three novel viruses, the RdRP amino acid sequence of each  
423 virus was aligned together with ~20 sequences of other viruses from the corresponding family.  
424 Representative sequences were chosen from a BLASTp search and from the supplementary  
425 material of Shi et al. 2016, to represent the whole family (or subfamily for the AnvRV). As the  
426 AnvDV and AnvIFV belong to the same *Picornavirales* order, one tree was constructed for both  
427 of them together. Multiple sequence alignment was conducted by Clustal Omega and a maximum  
428 likelihood tree was constructed with the LG substitution model using PhyML V.3 (Sievers et al.,  
429 2011) . Branch support was measured by approximate likelihood ratio tests (SH-aLRT; Guindon  
430 et al., 2010). The outgroups chosen for the AnvRV tree were two mammal infecting viruses from  
431 the subfamily *Sedoreovirinae*, and a poliovirus sequence was used for the *Picornavirales* tree.

#### 432 *Virion purification from Anagyrus vladimiri and Planococcus citri*

433 To test whether any of the three RNA viruses originate from the mealybug hosts, virions were  
434 purified from pools of: i) Mass-reared (MR) W<sup>+</sup> *A. vladimiri* (~0.7 g), ii) Field-collected *A.*  
435 *vladimiri* line without the AnvRV (RV<sup>-</sup>) (~0.2 g), iii) un-parasitized *P. citri*, (~0.7 g) and iv) *P.*  
436 *citri*, four days after parasitization by MR *A. vladimiri*, (~0.3 g) (see Table 1 for details).  
437 Purification was done according to Luria et al., (2020), with minor modifications. Briefly, the  
438 insects were homogenized in a TBE buffer, supernatant was filtered through a 0.45 µm membrane,  
439 placed on a 30% sucrose cushion, and subjected to ultracentrifugation at 242,922 g for 2 h. Then,  
440 RNA was extracted from the pellet using the Viral RNA extraction kit (Bioneer, Daejeon, South

441 Korea). Detection of the three viruses (AnvRV, AnvIFV and AnvDV) in those samples was carried  
442 by cDNA synthesis and PCRs as described below.

#### 443 *PCR detections of the three viruses*

444 Detection of RNA viruses in *A. vladimiri* individuals was obtained by RNA extraction (RNeasy  
445 plus kit, Qiagen, Düsseldorf, Germany) according to manufacturer protocol, with addition of  
446 Dithiothreitol to homogenizing buffer, to inhibit degradation by RNase. RNA samples were  
447 reverse-transcribed to cDNA using the RT-PCRbio kit (PCR Biosystems, London, UK), with no-  
448 template and no-enzyme controls. cDNA was used as templates for diagnostic PCR to identify  
449 presence/absence of the three viruses. Specific primers were designed for each virus and each viral  
450 genomic segment according to the contig sequences identified from the RNA-seq data (Supp. table  
451 1).

#### 452 *Transmission electron microscope (TEM)*

453 *Anagyrus vladimiri* females from the W<sup>+</sup>RV<sup>+</sup> line (see Table 1 for details) were used to test for the  
454 presence of viruses in the reproductive tissues of the parasitoids. Dissected *A. vladimiri* ovaries  
455 were fixed overnight with 1% Paraformaldehyde, 2.5% Glutaraldehyde in 0.1 M Cacodylate buffer  
456 pH 7.4 containing 5 mM CaCl<sub>2</sub>, washed in 0.1 M cacodylate, post fixed for 1 hour in with 1%  
457 OsO<sub>4</sub> and 5 mM CaCl<sub>2</sub> in Cacodylate buffer. Then the samples went through dehydration in  
458 ethanol and embedded in epon 812 (EMS). The blocks were cut with a diamond knife using a UC7  
459 ultramicrotome (Leica, Wetzlar, Germany). Sections of ~75nm were collected on grids, contrast  
460 stained for 10 min with 2% uranyl acetate and visualized in a TEM (L120C, Talos, Thermo Fisher  
461 Scientific, MA, USA).

## 462 References

- 463 Avidov, Z., Rosseler, Y., and Rosen, D. (1967). Studies on an Israel strain of *Anagyrus pseudococci*  
464 (Girault) [Hym., Encyrtidae]. II. Some biological aspects. *Entomophaga* 12, 111–118. doi:  
465 10.1007/BF02370607.
- 466 Blumberg, D. (1997). Parasitoid encapsulation as a defense mechanism in the Coccoidea (Homoptera) and  
467 its importance in biological control. *Biological Control* 8, 225–236. doi:10.1006/BCON.1997.0502.
- 468 Blumberg, D., Klein, M., and Mendel, Z. (1995). Response by encapsulation of four mealybug species  
469 (Homoptera: Pseudococcidae) to parasitization by *Anagyrus pseudococci*. *Phytoparasitica* 23, 157–  
470 163. doi:10.1007/BF02980975.

- 471 Bonning, B. C., and Miller, W. A. (2010). Dicistroviruses. *Annual Review of Entomology* 55, 129–150.  
472 doi:10.1146/ANNUREV-ENTO-112408-085457.
- 473 Bugila, A. A. A., Franco, J. C., da Silva, E. B., and Branco, M. (2015). Suitability of five mealybug species  
474 (Hemiptera, Pseudococcidae) as hosts for the solitary parasitoid *Anagyrus sp. nr. pseudococci*  
475 (Girault) (Hymenoptera: Encyrtidae). *Biocontrol Science and Technology* 25, 108–120.  
476 doi:10.1080/09583157.2014.952711.
- 477 Wu, C. Y., Zhao, Y. J., and Zhu, J. Y. (2021). Genome sequence of a novel member of the order  
478 *Picornavirales* from the endoparasitoid wasp *Diversinervus elegans*. *Archives of Virology* 166, 295–  
479 297. doi: 10.1007/s00705-020-04824-y.
- 480 Cheng, R. L., Li, X. F., and Zhang, C. X. (2021). Novel Dicistroviruses in an unexpected wide range of  
481 invertebrates. *Food and Environmental Virology* 13, 423–431. doi:10.1007/s12560-021-09472-2.
- 482 Coffman, K. A., Harrell, T. C., and Burke, G. R. (2020). A mutualistic Poxvirus exhibits convergent  
483 evolution with other heritable viruses in parasitoid wasps. *Journal of Virology* 94, e02059-19.  
484 doi:10.1128/JVI.02059-19.
- 485 Cogni, R., Ding, S. D., Pimentel, A. C., Day, J. P., and Jiggins, F. M. (2021). *Wolbachia* reduces virus  
486 infection in a natural population of *Drosophila*. *Communications Biology* 4, 1327.  
487 doi:10.1038/s42003-021-02838-z.
- 488 Deacutis, J. (2012). The characterization and biological effects of a novel cypovirus on the *Heliothis*  
489 *virescens* and *Campoletis sonorensis* host-parasitoid system. University of Kentucky.
- 490 Dheilly, N. M., Maure, F., Ravallec, M., Galinier, R., Doyon, J., Duval, D., et al. (2015). Who is the puppet  
491 master? Replication of a parasitic wasp-associated virus correlates with host behaviour manipulation.  
492 *Proceedings of the Royal Society B: Biological Sciences* 282, 20142773. doi:10.1098/rspb.2014.2773.
- 493 Drew, G. C., Stevens, E. J., and King, K. C. (2021). Microbial evolution and transitions along the parasite–  
494 mutualist continuum. *Nature Reviews Microbiology* 19, 623–638. doi:10.1038/s41579-021-00550-7.
- 495 Godfray, H. J. C. (1994). *Parasitoids : Behavioral and Evolutionary Ecology*. Princeton University Press.
- 496 Gottlieb, Y., Zchori-Fein, E., Mozes-Daube, N., Kontsedalov, S., Skaljic, M., Brumin, M., et al. (2010).  
497 The transmission efficiency of tomato yellow leaf curl virus by the whitefly *Bemisia tabaci* is  
498 correlated with the presence of a specific symbiotic bacterium species. *Journal of Virology* 84, 9310–  
499 9317. doi: 10.1128/jvi.00423-10.
- 500 Graham, R. I., Rao, S., Sait, S. M., Attoui, H., Mertens, P. P. C., Hails, R. S., et al. (2008). Sequence analysis  
501 of a reovirus isolated from the winter moth *Operophtera brumata* (Lepidoptera: Geometridae) and its  
502 parasitoid wasp *Phobocampe tempestiva* (Hymenoptera: Ichneumonidae). *Virus Research* 135, 42–  
503 47. doi:10.1016/j.virusres.2008.02.005.
- 504 Guindon, S., Dufayard, J. F., Lefort, V., Anisimova, M., Hordijk, W., and Gascuel, O. (2010). New  
505 algorithms and methods to estimate maximum-likelihood phylogenies: Assessing the performance of  
506 PhyML 3.0. *Systematic Biology* 59, 307–321. doi:10.1093/SYSBIO/SYQ010.
- 507 Hedges, L. M., Brownlie, J. C., O'Neill, S. L., and Johnson, K. N. (2008). *Wolbachia* and virus protection  
508 in insects. *Science* 322, 702–702. doi:10.1126/science.1162418.

- 509 Herniou, E. A., Huguet, E., Thézé, J., Bézier, A., Periquet, G., and Drezen, J.-M. (2013). When parasitic  
510 wasps hijacked viruses: genomic and functional evolution of polydnviruses. *Philosophical*  
511 *Transactions of the Royal Society B: Biological Sciences* 368, 20130051.  
512 doi:10.1098/RSTB.2013.0051.
- 513 Himler, A. G., Adachi-Hagimori, T., Bergen, J. E., Kozuch, A., Kelly, S. E., Tabashnik, B. E., et al. (2011).  
514 Rapid spread of a bacterial symbiont in an invasive whitefly is driven by fitness benefits and female  
515 bias. *Science* 332, 254–256. doi:10.1126/science.1199410.
- 516 Hoffmann, A. A., Montgomery, B. L., Popovici, J., Iturbe-Ormaetxe, I., Johnson, P. H., Muzzi, F., et al.  
517 (2011). Successful establishment of *Wolbachia* in *Aedes* populations to suppress dengue transmission.  
518 *Nature* 476, 454–457. doi:10.1038/nature10356.
- 519 IRESite: The database of experimentally verified IRES structures (2022).  
520 [http://www.iresite.org/IRESite\\_web.php?page=blastsearch&search\\_type=blast\\_iress](http://www.iresite.org/IRESite_web.php?page=blastsearch&search_type=blast_iress) [Accessed  
521 January 30, 2022].
- 522 Izraeli, Y., Lalzar, M., Mozes-Daube, N., Steinberg, S., Chiel, E., and Zchori-Fein, E. (2020). *Wolbachia*  
523 influence on the fitness of *Anagyrus vladimiri* (Hymenoptera: Encyrtidae), a bio-control agent of  
524 mealybugs. *Pest Management Science* 77, 1023–1034. doi:10.1002/ps.6117.
- 525 Khramtsov, N. v., Woods, K. M., Nesterenko, M. v., Dykstra, C. C., and Upton, S. J. (1997). Virus-like,  
526 double-stranded RNAs in the parasitic protozoan *Cryptosporidium parvum*. *Molecular Microbiology*  
527 26, 289–300. doi:10.1046/j.1365-2958.1997.5721933.x.
- 528 Kliot, A., Cilia, M., Czosnek, H., and Ghanim, M. (2014). Implication of the bacterial endosymbiont  
529 *Rickettsia* spp. in interactions of the whitefly *Bemisia tabaci* with tomato yellow leaf curl virus.  
530 *Journal of Virology* 88, 5652–5660. doi: 10.1128/jvi.00071-14.
- 531 Luria, N., Smith, E., Lachman, O., Laskar, O., Sela, N., and Dombrovsky, A. (2020). Isolation and  
532 characterization of a novel crivirus, the first Dicistroviridae family member infecting the cotton  
533 mealybug *Phenacoccus solenopsis*. *Archives of Virology* 165, 1987–1994. doi:10.1007/s00705-020-  
534 04702-7.
- 535 Lüthi, M. N., Vorburger, C., and Dennis, A. B. (2020). A Novel RNA Virus in the parasitoid wasp  
536 *Lysiphlebus fabarum*: Genomic structure, prevalence, and transmission. *Viruses* 12, 59. doi:  
537 10.3390/V12010059.
- 538 Marchler-Bauer, A., Derbyshire, M. K., Gonzales, N. R., Lu, S., Chitsaz, F., Geer, L. Y., et al. (2015).  
539 CDD: NCBI’s conserved domain database. *Nucleic Acids Research* 43, D222–D226.  
540 doi:10.1093/NAR/GKU1221.
- 541 Martinez, J., Lepetit, D., Ravallec, M., Fleury, F., and Varaldi, J. (2016). Additional heritable virus in the  
542 parasitic wasp *Leptopilina boulardi*: Prevalence, transmission and phenotypic effects. *Journal of*  
543 *General Virology* 97, 523–535. doi:10.1099/jgv.0.000360.
- 544 Matthijssens, J., Attoui, H., Bányai, K., Brussaard, C. P. D., Danthi, P., Vas, M., et al. (2022). ICTV Virus  
545 Taxonomy Profile: Reoviridae. *Journal of General Virology*.
- 546 Perlmutter, J. I., and Bordenstein, S. R. (2020). Microorganisms in the reproductive tissues of arthropods.  
547 *Nature Reviews Microbiology* 18, 97–111. doi:10.1038/s41579-019-0309-z.

- 548 Perreau, J., and Moran, N. A. (2022). Genetic innovations in animal–microbe symbioses. *Nature Reviews*  
549 *Genetics* 23, 23–39. doi: 10.1038/s41576-021-00395-z.
- 550 Renault, S., Bigot, S., Lemesle, M., Sizaret, P.-Y. Y., and Bigot, Y. (2003). The cypovirus *Diadromus*  
551 *pulchellus* RV-2 is sporadically associated with the endoparasitoid wasp *D. pulchellus* and modulates  
552 the defence mechanisms of pupae of the parasitized leek-month, *Acrolepiopsis assectella*. *Journal of*  
553 *General Virology* 84, 1799–1807. doi:10.1099/vir.0.19038-0.
- 554 Renault, S., Stasiak, K., Federici, B., and Bigot, Y. (2005). Commensal and mutualistic relationships of  
555 reoviruses with their parasitoid wasp hosts. *Journal of Insect Physiology* 51, 137–148.  
556 doi:10.1016/j.jinsphys.2004.08.002.
- 557 Shah, P. N. M., Stanifer, M. L., Höhn, K., Engel, U., Haselmann, U., Bartenschlager, R., et al. (2017).  
558 Genome packaging of reovirus is mediated by the scaffolding property of the microtubule network.  
559 *Cellular Microbiology* 19, e12765. doi:10.1111/cmi.12765.
- 560 Shi, M., Lin, X. D., Tian, J. H., Chen, L. J., Chen, X., Li, C. X., et al. (2016). Redefining the invertebrate  
561 RNA virosphere. *Nature* 540, 539–543. doi:10.1038/nature20167.
- 562 Sievers, F., Wilm, A., Dineen, D., Gibson, T. J., Karplus, K., Li, W., et al. (2011). Fast, scalable generation  
563 of high-quality protein multiple sequence alignments using Clustal Omega. *Molecular Systems*  
564 *Biology* 7, 539. doi:10.1038/MSB.2011.75.
- 565 Sorrentino, S., Carsana, A., Furia, A., Daskalov, J., and Libonati, M. (1980). Ionic control of enzymic  
566 degradation of double-stranded RNA. *Biochimica et Biophysica Acta* 609, 40–52. doi:10.1016/0005-  
567 2787(80)90199-9.
- 568 Suma, P., Mansour, R., Russo, A., La Torre, I., Bugila, A. A. A., and Franco, J. C. (2012). Encapsulation  
569 rates of the parasitoid *Anagyrus* sp. nr. *pseudococci*, by three mealybug species (Hemiptera:  
570 Pseudococcidae). *Phytoparasitica* 40, 11–16. doi:10.1007/s12600-011-0199-8.
- 571 Valles, S. M., Chen, Y., Firth, A. E., Guérin, D. M. A., Hashimoto, Y., Herrero, S., et al. (2017a). ICTV  
572 virus taxonomy profile: Dicistroviridae. *Journal of General Virology* 98, 355–356.  
573 doi:10.1099/JGV.0.000756.
- 574 Valles, S. M., Chen, Y., Firth, A. E., Guérin, D. M. A., Hashimoto, Y., Herrero, S., et al. (2017b). ICTV  
575 virus taxonomy profile: Iflaviridae. *Journal of General Virology* 98, 527–528.  
576 doi:10.1099/JGV.0.000757/CITE/REFWORKS.
- 577 Varaldi, J., Boulétreau, M., and Fleury, F. (2005). Cost induced by viral particles manipulating  
578 superparasitism behaviour in the parasitoid *Leptopilina boulardi*. *Parasitology* 131, 161–168.  
579 doi:10.1017/S0031182005007602.
- 580 Varaldi, J., Fouillet, P., Ravallec, M., López-Ferber, M., Boulétreau, M., and Fleury, F. (2003). Infectious  
581 behavior in a parasitoid. *Science* 302, 1930. doi:10.1126/science.1088798.
- 582 Varaldi, J., Gandon, S., Rivero, A., Patot, S., Fleury, F., Gandon, S., et al. (2006). “A newly discovered  
583 virus manipulates superparasitism behavior in a parasitoid wasp,” in *Insect Symbiosis*, ed. Bourtzis,  
584 K., and Miller, T. A. Taylor and Francis, (Boca Raton, FL: CRC Press), 141–162.  
585 doi:10.1201/9781420005936-11.

- 586 Walker, T., Johnson, P. H., Moreira, L. A., Iturbe-Ormaetxe, I., Frentiu, F. D., McMeniman, C. J., et al.  
587 (2011). The wMel *Wolbachia* strain blocks dengue and invades caged *Aedes aegypti* populations.  
588 *Nature* 476, 450–453. doi:10.1038/NATURE10355.
- 589 Webster, C. L., Longdon, B., Lewis, S. H., and Obbard, D. J. (2016). Twenty-Five new viruses associated  
590 with the Drosophilidae (Diptera). *Evolutionary Bioinformatics* 12, 13–25. doi:10.4137/EBO.S39454.
- 591 Wu, H., Pang, R., Cheng, T., Xue, L., Zeng, H., Lei, T., et al. (2020). Abundant and diverse RNA viruses  
592 in insects revealed by RNA-Seq analysis: Ecological and evolutionary implications. *mSystems* 5, 1–  
593 14. doi:10.1128/msystems.00039-20.
- 594 Zchori-Fein, E., and Bourtzis, K. (2011). *Manipulative Tenants; Bacteria Associated with Arthropods*.  
595 Boca Raton: CRC Press. doi:10.1201/b11008.
- 596 Zhang, J., Wang, F., Yuan, B., Yang, L., Yang, Y., Fang, Q., et al. (2021). A novel cripavirus of an  
597 ectoparasitoid wasp increases pupal duration and fecundity of the wasp's *Drosophila melanogaster*  
598 host. *The ISME Journal* 15, 3239-3257. doi:10.1038/s41396-021-01005-w.

599 Tables

**Table 1.** Summary of *Anagyrus vladimri* lines used in this study.

<i>line name</i>	<i>source</i>	<i>experiments used for</i>
<b>MR</b>	‘Biobee’ mass-rearing facility	Virome analysis
<b>W<sup>+</sup>RV<sup>+</sup></b>	‘Biobee’ mass-rearing facility, and further reared in our lab. Wasps carry <i>Wolbachia</i> and AnvRV.	Virus prevalence screening, Reovirus segment screening, Transmission electron microscopy
<b>W<sup>-</sup>RV<sup>+</sup></b>	MR wasps that fed on antibiotics (Izraeli <i>et al.</i> 2020) Wasps carry AnvRV but not <i>Wolbachia</i> .	Virus prevalence screening
<b>Field</b>	Field collections, north Israel	Virus prevalence screening, Reovirus segment screening (negative controls)
<b>Field-RV<sup>-</sup></b>	Iso-female lines of the field collected wasps	Presence of viruses in mealybugs

600 **Table 2.** Virome analysis of *A. vladimiri*. Details for all 30 contigs resulted from RNAseq.

contig name	contig length	ORF length	UTRs length	UTR/contig length	BLASTx hit	taxonomic group	amino acid identity (%)
k119_28	10031	9173	858	0.085535	YP_009111311.1	Iflaviridae	47
k119_29	8726	7829	897	0.102796	NP_620564.1	Dicistroviridae	38
k119_27	4250	4148	102	0.024	YP_392501.1	Reoviridae	33
k119_21	3936	3788	148	0.037602	QBA09478.1	Reoviridae	29
k119_25	3620	3521	99	0.027348	APG79179.1	Reoviridae	25
k119_19	3388	3257	131	0.038666	YP_392504.1	Reoviridae	45
k119_14	2163	1985	178	0.082293	YP_392505.1	Reoviridae	22
k119_18	1963	1388	575	0.292919		Reoviridae*	
k119_22	1880	1814	66	0.035106	QYV43128.1	Reoviridae	
k119_20	1865	1739	126	0.06756	AWA82241.1	Reoviridae	24
k119_12	1620	1526	94	0.058025	YP_392507**	Reoviridae	
k119_17	1535	1418	117	0.076221	QBA09478.1	Reoviridae	34
k119_24	1067	107	960	0.899719	XP_017796731.1	Hymenoptera	
k119_30	887	223	664	0.748591		NA	
k119_9	809	743	66	0.081582	YP_009342053.1	Iflaviridae	39
k119_10	782	311	471	0.602302		NA	
k119_16	711	0	711	1		NA	
k119_8	701	611	90	0.128388	YP_009342053.1	Iflaviridae	40
k119_15	571	437	134	0.234676	CAB0037418.1	Hymenoptera	
k119_2	564	389	175	0.310284	XP_015596585.1	NA	
k119_4	560	230	330	0.589286	EZA52908.1	Hymenoptera	
k119_7	451	320	131	0.290466	CAA84692.1	Phage	
k119_13	432	203	229	0.530093	YP_009342053.1	Iflaviridae	
k119_6	412	83	329	0.798544		NA	
k119_5	394	356	38	0.096447	QFP98431.1	Iflaviridae	36
k119_3	375	371	4	0.010667	YP_009342053.1	Iflaviridae	
k119_0	358	143	215	0.600559	ABD33943.1	Picornaviriales	
k119_23	351	86	265	0.754986	AGF91671.1	Phage	
k119_26	306	296	10	0.03268	QGJ03578.1	Phage	
k119_1	218	164	54	0.247706	YP_009342053.1	Iflaviridae	

601 \*concluded as part of the genome of AnvRV by the segment screening assay (see table 3)

602 \*\*this hit was found only by using the PSI-BLASTp algorithm



603 **Table 3.** Screening of ten AnvRV segments in 24 individuals from two lines of *A. vladimiri*; 16  
 604 females from the MR population, and eight from Field population. ‘0’ denotes absence, ‘+’ denotes  
 605 presence of the viral genomic segment by diagnostic PCR. Empty boxes denote untested samples.

Contig	Homologous ObIRV segment	Mass-reared population																Field population							
		1	2	3	4	5	6	7	8	9	10	11	12	13	14	15	16	1	2	3	4	5	6	7	8
k119_27	segment1	+	+	+	+	+	+	+	+	+	+	+	+	+	+	+	+	0	0	0	0	0	0	0	0
k119_21	segment2	+	+	+	0	+	+	+	+	+	+	0	+	+	+	0	0	0	0	0	0	0	0	0	0
k119_25	segment3	+	+	+	+	+	+	+	+	+	+	+	+	+	+	+	+	0	0	0	0	0	0	0	0
k119_19	segment4	+	+	+	+	+	+	+	+	+	+	+	+	+	+	+	+	+	0	0	0	0	0	0	+
k119_14	segment5	+	+	+	0	+	+	+	0	+	+	+	+	0	+	+	+	0	0	0	0	0	0	0	0
k119_20	segment6	+	+	+	+	+	+	+	+	+	+	+	+	+	+	+	+	0	0	0	0	0	0	0	0
k119_12	segment7	+	+	+	+	+	+	+	+	+	+	+	+	+	+	+	+	0	0	0	0	0	0	0	0
k119_17	segment8	+	+	+	+	+	0	+	+	+	+	+	+	0	+	+	+	0	0	0	0	0	0	0	0
k119_22	segment10	+	+	+	+	+	+	+	0	+	+	+	+	+	+	+	+	0	0	0	0	0	0	0	0
k119_18	Unknown	+	+	+	+	+	+	+	+	+				0	+	+	+	0	0	0	0	0	0	0	0

606

## 607 Figure legends

608 **Fig 1.** Electrophoresis pattern (using a 0.8% agarose gel) of VNAs extracted from *A. vladimiri*,  
609 which were treated by RNase and DNase separately. ‘AV’ denotes VNAs of *A. vladimiri*. ‘SSC’  
610 denotes sodium citrate buffer, which was used in 0.01x and 2x ionic strengths. ‘10’/‘0.1’ denotes  
611 high/low concentration ( $\mu\text{g/ml}$ ) of RNase respectively. Details by lane numbers: 1-3; no digestion  
612 treatment. 1; 1Kb ladder (1KB+, Invitrogen, MA, USA), 2; Phi6 – a ladder made of viral dsRNA  
613 (Invitrogen, MA, USA), 3; *A. vladimiri* VNA. 4-11; Digestion by RNase A in four buffer/enzyme  
614 concentrations. 4-7; Phi6 ladder as a control for the enzymatic activity of RNase. 8-11; AV  
615 digestion. 12-13; Digestion by DNase I, 12; 1Kb – a DNA ladder as a control for the enzymatic  
616 activity of DNase. 13; AV digestion.

617 **Fig 2.** Virome analysis of *A. vladimiri*. The assembled 30 contigs were assigned to seven  
618 taxonomic groups according to the best BLASTx hit. **A)** Average depth per taxonomic group,  
619 calculated as:  $((\text{sum number of reads} * 100\text{bp}) / \text{sum length of contigs})$ . **B)** Columns represent the size of  
620 each of the 30 contigs (bp length). Purple crosses represent the proportion of both 5’ and 3’  
621 untranslated regions (UTRs) to the contigs’ full length, as predicted by the ORF finder. High  
622 proportion suggests insufficient protein products, while low proportion suggests a true protein is  
623 translated from this contig. See table 2 for more details about each contig.

624 **Fig 3.** Genome annotation of the three novel RNA viruses. **A)** AnvDV and AnvIFV. White box indicates  
625 location of ORF, colored boxes indicate identified protein domains. Numbers on scale are in bp according  
626 to the full contig. RdRP, RNA-dependent RNA polymerase. **B)** Annotation of the segmented AnvRV.  
627 The ten segments are drawn to scale, with boxes indicating the ORF location on the full segment, colors  
628 represent the proteins encoded from those segments as assigned from homology to known sequences of the  
629 ObIRV genome.

630 **Fig 4.** Phylogenetic analysis of AnvRV (colored), based on amino acid sequence similarities of the RdRP  
631 genome segment (~1,200aa long). Representative viruses of all nine genera in the subfamily  
632 Spinareovirinae are shown. The icons of organisms on the tips represent the taxonomic group of the host in  
633 which the virus was found. The ● symbol indicate viruses that have not been classified to the genus level.  
634 The human Rotavirus B and the bovine Bluetongue virus (Family: *Reoviridae*, subfamily: *Sedoreovirinae*)  
635 were used as an outgroup. The tree was inferred by maximum-likelihood using the LG substitution model,  
636 the numbers on branches indicate the results of approximate likelihood ratio tests for branch support (aLRT-  
637 SH test; Guindon et al. 2010). Scale bar: 0.7 substitutions per site.

638 **Fig 5.** Phylogenetic analysis of *A. vladimiri* iflavivirus (AnvIFV) and *A. vladimiri* dicistrovirus  
639 (AnvDV) (both colored), based on amino acid sequence similarities of the RdRP gene (~300aa  
640 long). The human poliovirus (order: *Picornavirales*, family: *Picornaviridae*) was used as an out-  
641 group. The icons of organisms on the tips represent the taxonomic group of the host in which the  
642 virus was found (however, in some cases the viruses can be found in hosts from additional arthro-  
643 pod orders, such as Cricket paralysis virus). The ‘star of David’ symbol signs the virus that is  
644 reported to have a mutualistic relationship with its insect host. The phenotype of all other viruses  
645 is either unknown or pathogenic. The tree was inferred by maximum-likelihood using the LG

646 substitution model, the numbers on branches indicate the results of approximate likelihood ratio  
647 tests for branch support (aLRT-SH test; Guindon et al. 2010). Scale bar: 0.5 substitutions per site.

648 **Fig 6.** The multi-infection status of three lines of *A. vladimiri* individuals by the three RNA viruses  
649 and *Wolbachia*. Boxes on the same horizontal axis denote the infection status of the four microbes  
650 in the same individual; blue fill=detected, no fill=undetected. Detection of the AnvRV, which has  
651 a segmented genome, was done with the primers targeted to the largest segment, encoding for the  
652 RdRp gene (see supp. table 1 for all primer pairs used). W+: wasps from the *Wolbachia*-infected  
653 line, W-: wasps from *Wolbachia*-uninfected line.

654 **Fig 7.** Transmission electron microscope images of AnvRV particles in *A. vladimiri* follicle cells.  
655 **A)** a cluster of virus particles (black arrow), **B)** a viroplasm (Vp), **C)** high magnification of a small  
656 cluster of virions. N, nucleus; M, mitochondria. Scale bars; A) 500 nm, B) 500nm, C) 100nm.

## 657 Data availability

658 **Accession numbers to be received.**

## 659 Conflict of interest declaration

660 Author SS was employed by BioBee Sde Eliyahu Ltd. The remaining authors declare that the  
661 research was conducted in the absence of any commercial or financial relationships that could be  
662 construed as a potential conflict of interest.

## 663 Acknowledgements

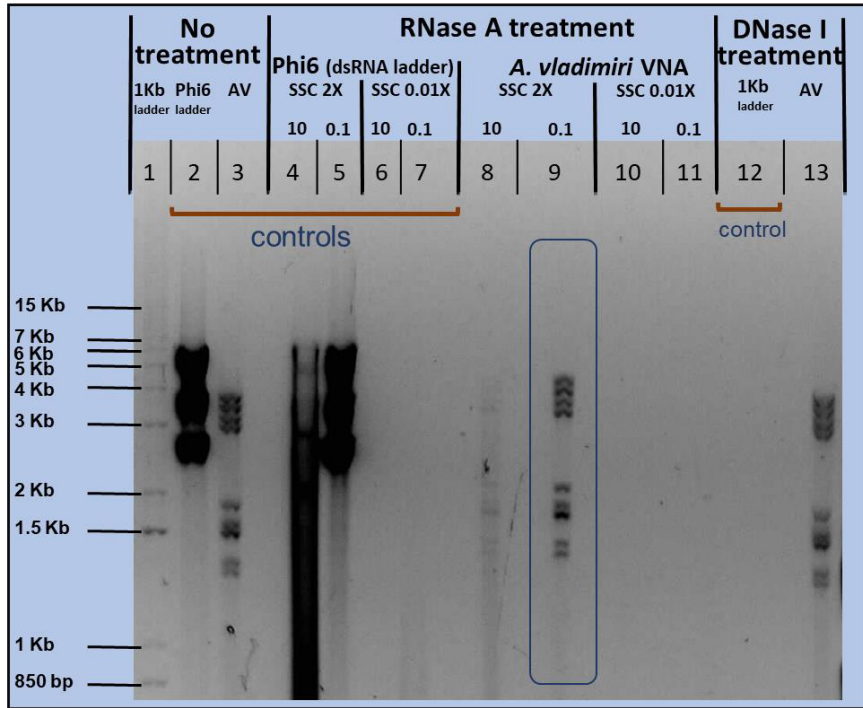
664 The authors would like to thank Prof. A. Dombrovsky for useful advice, E. Erel for insect rearing  
665 consultancy and Dr. L. Shaulov for preparation and visualization of ovary slides in TEM.

## 666 Funding

667 This research was supported by the ISRAEL SCIENCE FOUNDATION (grant No. 397/21) to E.  
668 Z-F and E.C.

1 Figures

2 Fig 1



3

4 **Fig 1.** Electrophoresis pattern (using a 0.8% agarose gel) of VNAs extracted from *A. vladimiri*, which were treated by RNase and DNase separately.  
 5 'AV' denotes VNAs of *A. vladimiri*. 'SSC' denotes sodium citrate buffer, which was used in 0.01x and 2x ionic strengths. '10'/'0.1' denotes high/low  
 6 concentration ( $\mu\text{g/ml}$ ) of RNase respectively. Details by lane numbers: 1-3; no digestion treatment. 1; 1Kb ladder (1KB+, Invitrogen, MA, USA), 2;  
 7 Phi6 – a ladder made of viral dsRNA (Invitrogen, MA, USA), 3; *A. vladimiri* VNA. 4-11; Digestion by RNase A in four buffer/enzyme concentrations.  
 8 4-7; Phi6 ladder as a control for the enzymatic activity of RNase. 8-11; AV digestion. 12-13; Digestion by DNase I, 12; 1Kb – a DNA ladder as a  
 9 control for the enzymatic activity of DNase. 13; AV digestion.

10

11

Fig 2

**A**

Taxonomic Group	Average Depth
Reoviridae	8
Iflaviridae	12621
NA	234
Hymenoptera	16
Phage	348
Dicistroviridae	307

**B**

Contig ID	Contig Length (bp)	UTR/contig_length
k119_28	~10000	~0.1
k119_29	~9000	~0.1
k119_27	~4200	~0.1
k119_21	~3800	~0.1
k119_25	~3500	~0.1
k119_19	~3200	~0.1
k119_14	~2200	~0.15
k119_18	~2000	~0.25
k119_22	~1800	~0.1
k119_20	~1700	~0.1
k119_12	~1600	~0.1
k119_17	~1500	~0.1
k119_24	~1200	~0.9
k119_30	~1000	~0.1
k119_9	~800	~0.1
k119_10	~700	~0.55
k119_16	~600	~0.95
k119_8	~500	~0.15
k119_15	~400	~0.25
k119_2	~300	~0.3
k119_4	~250	~0.55
k119_7	~200	~0.3
k119_13	~180	~0.5
k119_6	~150	~0.75
k119_5	~120	~0.15
k119_3	~100	~0.1
k119_0	~80	~0.55
k119_23	~70	~0.7
k119_26	~50	~0.1
k119_1	~40	~0.25

12

13 **Fig 2.** Virome analysis of *A. vladimiri*. The assembled 30 contigs were assigned to seven taxonomic groups according to the best BLASTx hit. **A)**  
 14 Average depth per taxonomic group, calculated as: ((sum number of reads\*100bp)/sum length of contigs). **B)** Columns represent the size of each of the 30  
 15 contigs (bp length). Purple crosses represent the proportion of both 5' and 3' untranslated regions (UTRs) to the contigs' full length, as predicted by  
 16 the ORF finder. High proportion suggests insufficient protein products, while low proportion suggests a true protein is translated from this contig.  
 17 See table 2 for more details about each contig.

18

Fig 3

**A**

AnvIFV: 532 to 9705 bp. Domains: Capsid (rhv like, cd00205), Capsid (CRPV superfamily, cl07393), RNA helicase (pfam00910), RdRP (cd01699).

AnvDV: 664 to 8493 bp. Domains: RNA helicase (pfam00910), RdRP (cd01699), Capsid (rhv like, cd00205), Capsid (CRPV superfamily, cl07393).

**B**

AnvRV segments (0 to 4000 bp scale):

- seg1: RdRP (blue)
- seg2: unknown (green)
- seg3: unknown (green)
- seg4: polyhedrin (red)
- seg5: unknown (green)
- seg6: unknown (green)
- seg7: unknown (green)
- seg8: unknown (green)
- seg9: unknown (green)
- segment10: unknown (green)

Protein legend: polyhedrin (red), RdRP (blue), unknown (green).

19

20 **Fig 3.** Genome annotation of the three novel RNA viruses. **A)** AnvDV and AnvIFV. White box indicates location of ORF, colored boxes indicate identified protein  
 21 domains. Numbers on scale are in bp according to the full contig. RdRP, RNA-dependent RNA polymerase. **B)** Annotation of the segmented AnvRV. The ten  
 22 segments are drawn to scale, with boxes indicating the ORF location on the full segment, colors represent the proteins encoded from those segments as assigned  
 23 from homology to known sequences of the ObIRV genome.

24

Fig 4

**Subfamily Spinareovirinae**

**Subfamily Sedoreovirinae**

0.7

**Legend**

- Diptera
- Hymenoptera
- Lepidoptera
- Hemiptera
- Arachnida
- Fish
- Mammalia
- Fungi
- Plantae

25

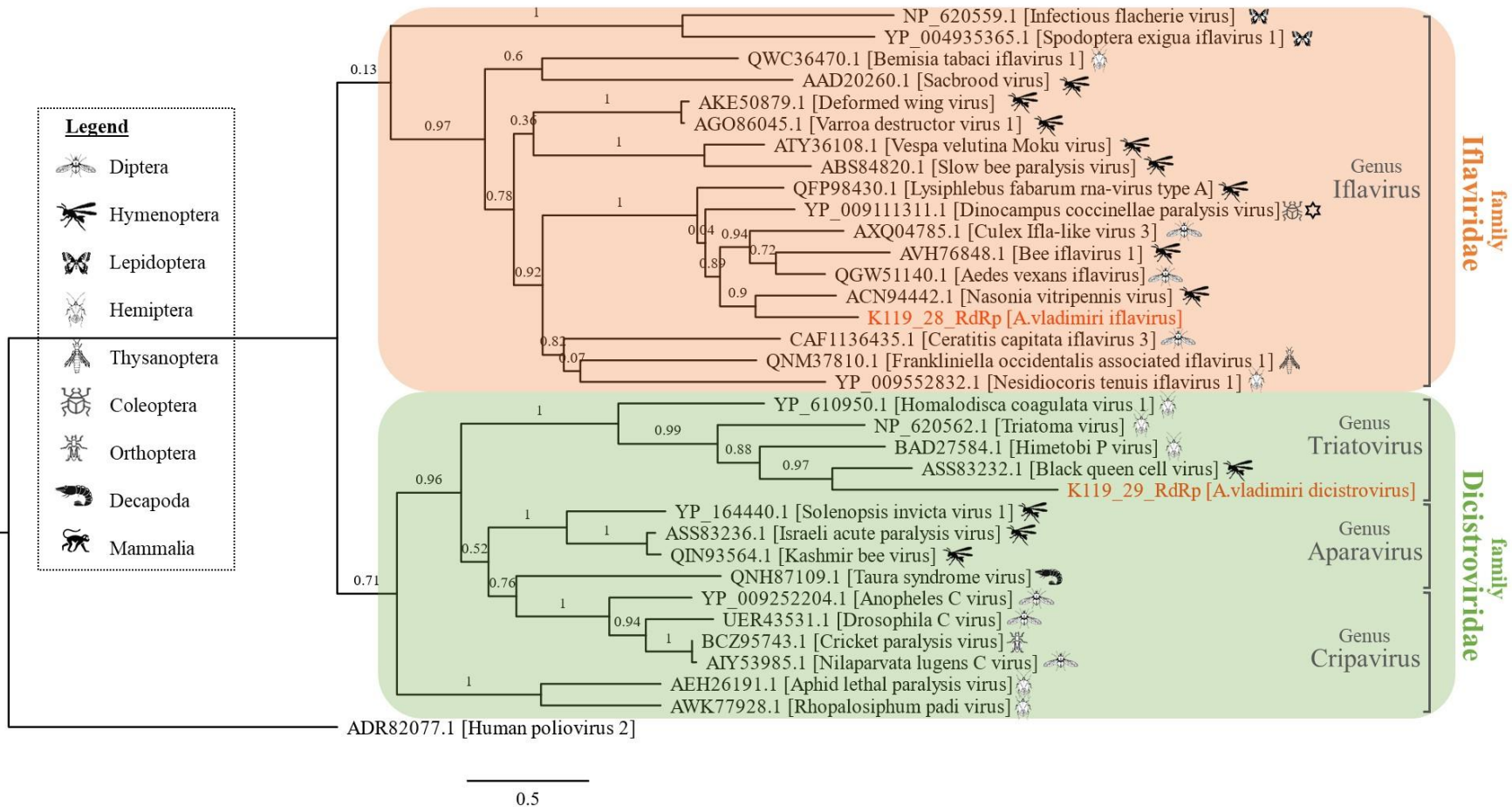
26 **Fig 4.** Phylogenetic analysis of AnRV (colored), based on amino acid sequence similarities of the RdRP genome segment (~1,200aa long). Representative viruses

27 of all nine genera in the subfamily Spinareovirinae are shown. The icons of organisms on the tips represent the taxonomic group of the host in which the virus was

28 found. The ● symbol indicate viruses that have not been classified to the genus level. The human Rotavirus B and the bovine Bluetongue virus (Family: *Reoviridae*,

29 subfamily: *Sedoreovirinae*) were used as an outgroup. The tree was inferred by maximum-likelihood using the LG substitution model, the numbers on branches

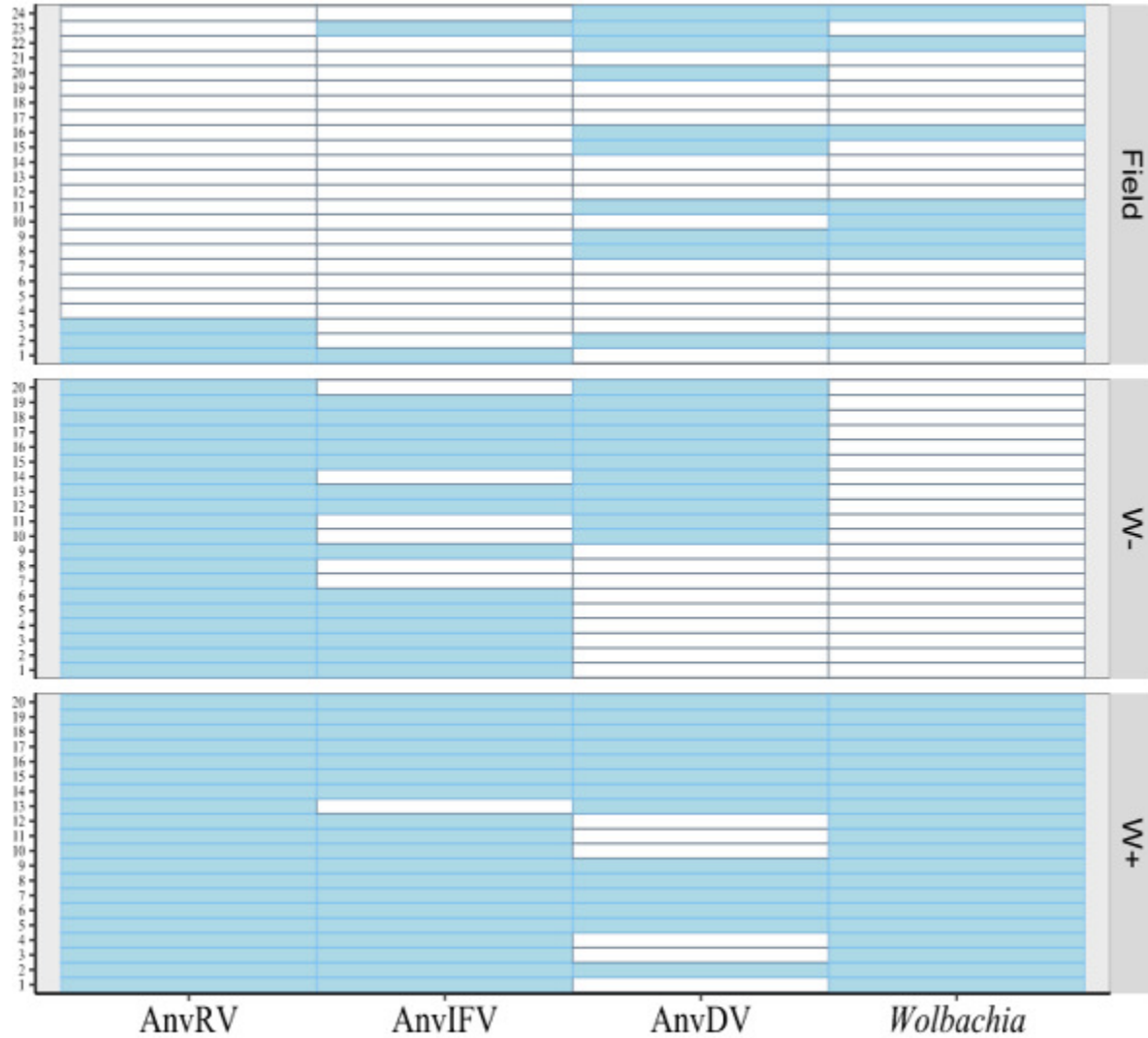
30 indicate the results of approximate likelihood ratio tests for branch support (aLRT-SH test; Guindon et al. 2010). Scale bar: 0.7 substitutions per site.



32

33 **Fig 5.** Phylogenetic analysis of *A. vladimiri* iflavivirus (AnvIFV) and *A. vladimiri* dicistrovirus (AnvDV) (both colored), based on amino acid sequence  
 34 similarities of the RdRP gene (~300aa long). The human poliovirus (order: *Picornavirales*, family: *Picornaviridae*) was used as an outgroup. The icons  
 35 of organisms on the tips represent the taxonomic group of the host in which the virus was found (however, in some cases the viruses can be found in  
 36 hosts from additional arthropod orders, such as Cricket paralysis virus). The ‘star of David’ symbol signs the virus that is reported to have a mutualistic  
 37 relationship with its insect host. The phenotype of all other viruses is either unknown or pathogenic. The tree was inferred by maximum-likelihood  
 38 using the LG substitution model, the numbers on branches indicate the results of approximate likelihood ratio tests for branch support (aLRT-SH test;  
 39 Guindon et al. 2010). Scale bar: 0.5 substitutions per site.

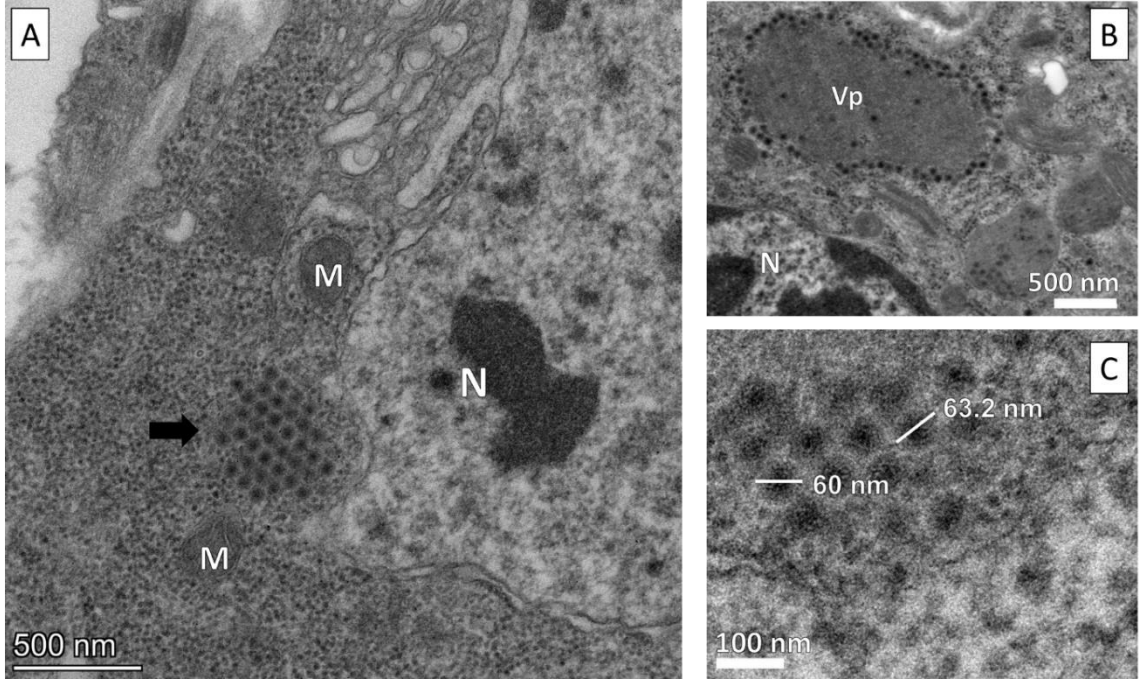




42 **Fig 6.** The multi-infection status of three lines of *A. vladimiri* individuals by the three RNA viruses and *Wolbachia*. Boxes on the same horizontal axis  
 43 denote the infection status of the four microbes in the same individual; blue fill=detected, no fill=undetected. Detection of the AnvRV, which has a  
 44 segmented genome, was done with the primers targeted to the largest segment, encoding for the RdRp gene (see supp. table 1 for all primer pairs used).  
 45 W+: wasps from the *Wolbachia*-infected line, W-: wasps from *Wolbachia*-uninfected line.

46

Fig 7



47

48

49

**Fig 7.** Transmission electron microscope images of AnvRV particles in *A. vladimiri* follicle cells. **A)** a cluster of virus particles (black arrow), **B)** a viroplasm (Vp), **C)** high magnification of a small cluster of virions. N, nucleus; M, mitochondria. Scale bars; A) 500 nm, B) 500nm, C) 100nm.

51